

## Invited

## Tilted Superlattices and Quantum Well Wire Arrays

Masahiro TSUCHIYA, Pierre M. PETROFF, and Larry A. COLDREN  
 Department of Electrical and Computer Engineering and Material Department  
 University of California, Santa Barbara, CA, 93106, USA

Fine sub-monolayer epitaxy on vicinal substrates offers possibility of fabricating well wires (QWW's). Using molecular beam epitaxy (MBE), periodic lateral heterostructures of nm dimensions named tilted superlattices (TSL's) have been successfully demonstrated. The TSL-growth has several significant advantages for making QWW structures and devices; (a) the low nm dimensions, (b) absence of damage, surface, and carrier depletion, and (c) no processing. In this paper, the growth of the TSL's by MBE, the optical properties of the QWW arrays, and the first lasers with QWW array active regions are described.

## 1. Introduction

Quantum well *wires* (QWW's) and quantum well *boxes* (QWB's) are attractive future materials beyond quantum well (QW) *layer* structures.<sup>1-3)</sup> Hence, quantum confinement in the lateral direction in a wafer plane in addition to the vertical is one of the hottest issues in the heterostructure physics and devices.<sup>1-11)</sup>

Fine sub-monolayer epitaxy on vicinal substrates,<sup>5)</sup> as shown in Fig. 1, offers possibilities of making QWW's. Using molecular beam epitaxy<sup>12,13)</sup> (MBE) or metal-organic chemical vapor deposition,<sup>14,15)</sup> periodic lateral structures named tilted superlattices (TSL's), indeed, have been successfully demonstrated. In comparison with the fine lithography techniques, the TSL-growth has several significant advantages: (a) the lateral dimensions are, in principle, in the low nm range which is suitable for obtaining sufficient quantum size effect and for making the QWW devices, (b) QWW arrays are free from damage, surface, and carrier depletion which are supposed to be problems in actual devices, and (c) this is presently the only processing-free method for fabricating QWW's

## 2. Tilted Superlattices

## 2.1 MBE Growth of TSL's

GaAs-AlGaAs TSL's can be achieved by alternating sub-monolayer deposition of  $(\text{GaAs})_m/-$

$(\text{AlAs})_n$  on a (100) GaAs vicinal substrates as shown in Fig. 1. The tilt parameter  $p$  ( $p = m+n$ ) should be unity. Since large atom mobility on step ledges and nucleation only at step risers are required, the sub-monolayer superlattices are deposited by alternate beams of (Ga or Al)/As (migration enhanced epitaxy MEE).<sup>16,17)</sup> The direction of the wafer tilt is usually [011]. The substrate temperature is around 600°C, where the step flow mode takes place even in a conventional MBE growth. Al composition modulation has been clearly observed by transmission electron microscopy (TEM) cross section in the TSL's thus grown.

In comparison with conventional QW layers, however, the structural quality of TSL's in the present stage still requires the following improvements:

## (a) Step Uniformity:

The size of the lateral structure is equal to the ledge size  $L_s$  of steps with one monolayer height ( $= a_0$ ), which is determined by

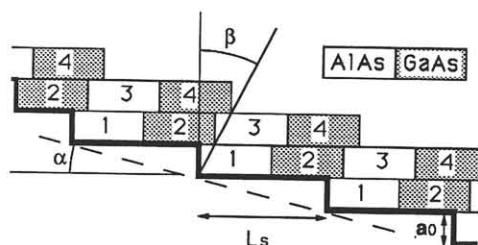


Fig. 1 Schematic of TSL's. The numbers in the rectangles show the order of the sub-monolayer depositions.

$$L_s = a_0 (\tan\alpha)^{-1} \quad (1),$$

where  $\alpha$  is the vicinal surface misorientation angle. (See Fig. 1.). Hence, the fluctuation in  $\alpha$  will affect severely the size of lateral heterostructures, leading to quantum energy fluctuations. For example, a variation  $\Delta\alpha$  of  $0.1^\circ$  around  $\alpha = 1^\circ$  gives  $\Delta L_s = 15 \text{ \AA}$ . Careful preparation of vicinal surfaces and suitable buffer layers are necessary.

**(b) Tilt Angle Control:**

The tilt angle  $\beta$  of a TSL with respect to the vertical is a function of  $p$  (monolayer/cycle) with

$$\beta = \tan^{-1} \left( \frac{p-1}{\tan\alpha} \right) \quad (2).$$

As shown in Fig. 2, the smaller  $\alpha$  is, the more difficult it is to obtain a vertical TSL ( $\beta = 0^\circ$ ). For instance, in order to achieve  $\beta$  within  $30^\circ$  on  $1^\circ$  off surfaces, the error in  $p$  is required to be less than 0.01 monolayer/cycle. This could be beyond the controllability of the present MBE machines.

**(c) Interface Abruptness:**

Abrupt heterointerfaces are necessary for the control of electronic and optical properties in TSL's. To obtain abrupt interfaces, nucleation only at step risers and straight line step edges are required. These features are supposed to be dominated by the kinetics and nucleation mechanism during the MBE growth.

**(d) Interface Smoothness:**

The conditions mentioned above in (b) and (c) have to be maintained during the whole TSL growth. Typical periods of the growth cycle are 10 - 100. Stable beam fluxes and precise and reproducible action of effusion cell shutters are necessary.

All the subjects in (a) - (d) might require the next generation of MBE machines as well as a better understanding of the MBE growth mechanism and optimization of the growth conditions.

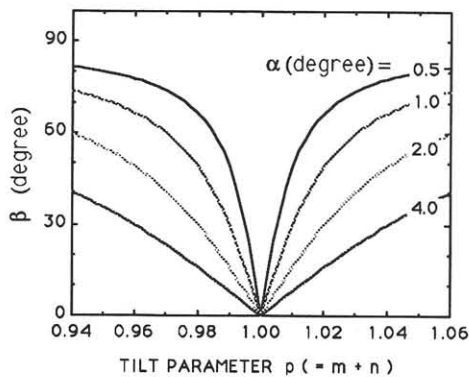


Fig. 2 Tilt angle  $\beta$  in TSL's on various vicinal surfaces of off angle  $\alpha$  are plotted as a function of tilt parameter  $p$ .

**2.2 Coherent TSL's**

Recently, we have observed a novel phenomenon: the formation of coherent TSL's (C-TSL's),<sup>18</sup> which is an evidence that kinetics and nucleation of atoms actually play very important roles during the TSL growth.

Periodic Al composition modulations named C-TSL (Fig. 3) have been observed to occur spontaneously during MBE growth of  $\text{Al}_x\text{Ga}_{1-x}\text{As}$  ( $x = 0.2 - 0.3$ ) on vicinal (100) substrates. The C-TSL is formed in the coherent MEE mode for which one monolayer of Al and Ga atoms are simultaneously deposited. Through a detailed TEM analysis of samples grown on various conditions, the following facts have been clarified; (a) the C-TSL formation is independent of Al composition in underlayers, (b) the C-TSL is formed before As flux is established, (c) Al rich regions are formed at the bottom of the steps, and (d) C-TSL's were observed in the layers grown at  $550^\circ\text{C}$  and  $600^\circ\text{C}$  while there is no TSL in the layer grown at  $650^\circ\text{C}$ .

The C-TSL formation shows that the kinetic and bonding behavior of Al atoms<sup>19</sup> is different from that of Ga atoms on the TSL growth condition, suggesting that in order to make high quality TSL's, an optimum growth condition have to be chosen for each element.

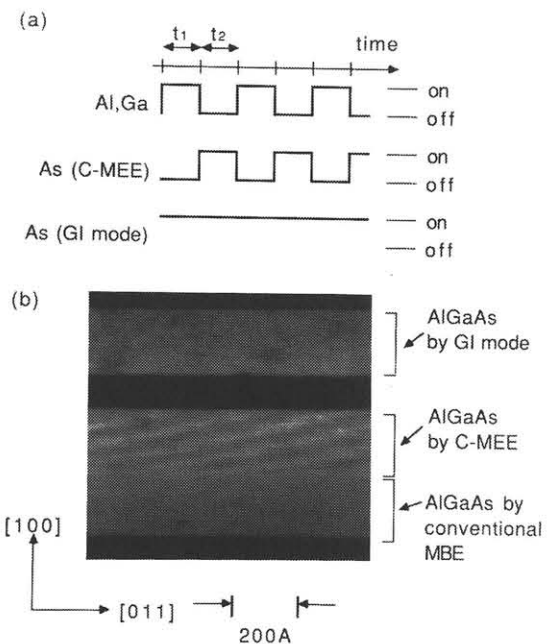


Fig. 3 (a) Schematic of the shutter opening and closing sequences for the C-MEE mode and for the growth interruption (GI) mode where growth interruption is introduced after each one monolayer MBE deposition of Al and Ga with As flux.

(b) Dark field TEM cross section micrograph of AlGaAs layers grown on a  $1^\circ$  off wafer by MBE, in the C-MEE mode, and in the GI mode. The Al rich regions correspond to the lighter areas in the micrograph.

### 3. Optical Properties of QWW arrays

We have succeeded in making QWW arrays using TSL's.<sup>9)</sup> In order to avoid the problems in the former section, QWW arrays shown in Fig. 4 was designed. In this structure,<sup>20,21)</sup> carriers are expected to be pushed from the TSL region to the GaAs layer and be confined laterally by the potential variation of the TSL ( $\sim 4$  nm GaAs/ 4 nm AlAs). Quantum level broadening due to the step size fluctuation is expected to be smaller because of the relatively weak lateral confinement as compared to QWW's with fully surrounding barriers.

In a single layer of the QWW array which was fabricated on a vicinal (001) semi-insulating GaAs substrate tilted  $2^\circ$  toward [110], we measured photoluminescence excitation (PLE) spectra at 1.4 K as a function of the in-plane polarization angle  $\theta$  of the excitation light. The average step size is 8 nm in this sample. Strong anisotropy of the ratio of electron light hole exciton peak ( $I_{1elh}$ ) to electron heavy hole exciton peak ( $I_{1ehh}$ ) has been observed, whereas no polarization dependence was found in a single quantum well sample. The variation of  $I_{1elh}/I_{1ehh}$  with  $\theta$  is plotted in Fig. 5.

A first order theory<sup>9)</sup> incorporating the optical selection rule<sup>22)</sup> for two dimensional quantum confinement is found to agree very well with the measured data as shown in Fig. 5. For a one dimensional exciton, a ratio of  $I_{1elh}/I_{1ehh}$  is given by the expression;

$$I_{1elh}/I_{1ehh} = \frac{[\frac{1}{2}|E_p|^2 + \frac{5}{4}|E_n|^2]}{[\frac{3}{2}|E_p|^2 + \frac{3}{4}|E_n|^2]} \quad (3).$$

Here,  $E_p$  and  $E_n$  are the electric field components parallel and normal to the QWW's, respectively. The fractions in front of  $|E_p|^2$  and  $|E_n|^2$  show the relative intensity of optical transitions of the 1elh and 1ehh excitons.

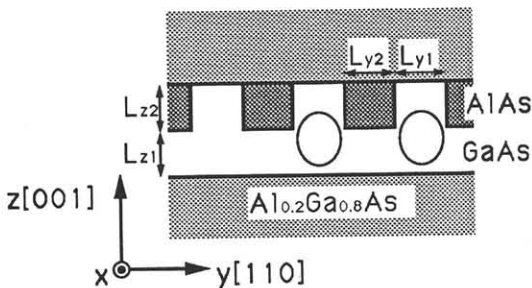


Fig. 4. Schematic illustration of the QWW array. It was designed to have  $L_{z1} = L_{z2} = 5$  nm,  $L_{y1} = L_{y2} = 4$  nm.

It was the first report of the in-plane anisotropy of PLE from QWW's. The data show that such TSL-QWW structures have great promise for use in novel optical devices.

### 4. SCH Lasers with QWW arrays

High performance of electronic and optical devices with QWW's have been expected.<sup>1-3,23-25)</sup> In the present stage, the TSL growth is the only way to introduce the dimensions required to realize the predicted superior properties of such QWW devices. We have made an attempt at fabricating lasers with QWW array active regions in order to see how such kind of QWW's work as laser materials.

#### 4.1 Fabrication of QWW Lasers

Separate-confinement-heterostructure (SCH) lasers having TSL-QWW's as active regions were fabricated. The TSL-QWW's consist of a 5 nm GaAs layer and a 5 nm {AlGaAs ( $x = 0.25$ ) - GaAs} TSL layer which are sandwiched by AlGaAs ( $x = 0.25$ ) waveguide layers and AlGaAs ( $x = 0.5$ ) cladding layers. The half-confined QWW was used again to avoid energy fluctuation due to the lateral size fluctuations. An in-plane polarization dependence of

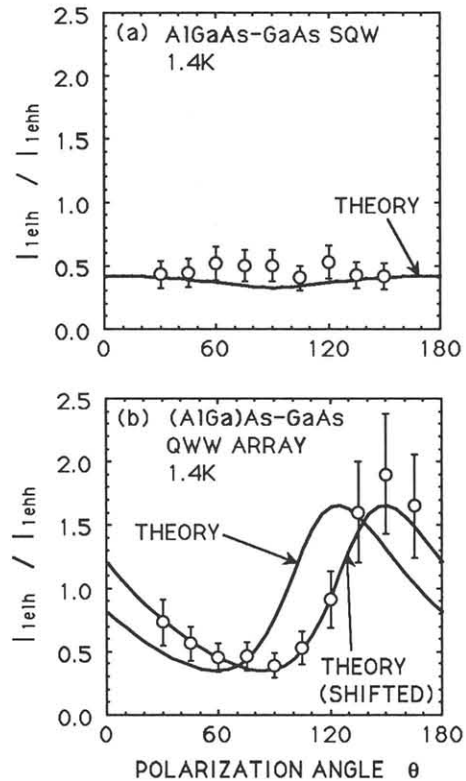


Fig. 5. The ratio of PLE peak for electron-light hole exciton ( $I_{1elh}$ ) to that for electron heavy hole exciton ( $I_{1ehh}$ ) is plotted as a function of the polarization angle  $\theta$  in the SQW sample (a) and in the QWW sample (b). The solid lines show the calculated prediction. The broken line in (b) is shifted from the theoretical curve by an offset of  $\Delta\theta = 25^\circ$ .

absorption was observed in the PLE spectra of the sample, indicating a presence of two dimensional quantum confinement in the QWW array.

#### 4.2 Basic Performance of the Lasers

Threshold current density as low as  $460 \text{ A/cm}^2$  and differential quantum efficiency of 29 % per facet were obtained in a laser thus fabricated with a long cavity ( $1120 \mu\text{m}$ ) at room temperature. The lasing wavelength was  $827 \text{ nm}$  which corresponds to the QWW state energy. Typical data are shown in Fig. 6. Measured modal gain spectra were as narrow as those of typical single QW lasers. Characteristic temperatures  $T_0$  were  $80 - 130^\circ\text{K}$ . Such a low values could be attributed to the relatively low thermal barriers in our QWW's. Although superior properties of QWW lasers were not observed, due to both nonoptimal device geometry and MBE growth parameters, the quality of the QWW array active region is still high enough to demonstrate good lasers.

#### 5. Summary

We have described above an attempt at making QWW's and QWW devices using TSL's. The quality of the QWW's and the performance of the devices are

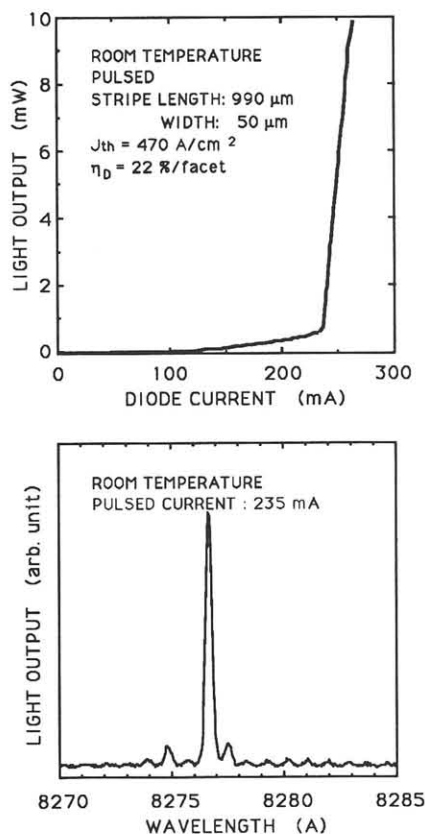


Fig. 6. L-I curve of a laser with the QWW array active region (a). Lasing spectra of the laser just above the threshold (b).

depending on the quality of TSL's, which still needs several improvements at present. Hence, further understanding of MBE, especially of MEE, and realization of ultra fine MBE machines are key points to upgrade the QWW's and devices with TSL's.

#### 6. Acknowledgment

The authors would like to thank Dr. J. M. Gaines for useful discussions. Thanks are also due to J. H. English, R. J. Simes, and R. S. Geels for their support in the MBE growth and due to T. Y. Liu and Y. Li for their help in the TEM analysis. This work was supported in part by the Innovative Science & Technology Directorate of SDIO via ARO and ONR, and through the QUEST NSF Science and Technology Center.

#### References

- 1) H. Sakaki: Jpn. J. Appl. Phys. **19**(1980) 94.
- 2) Y. Arakawa and H. Sakaki: Appl. Phys. Lett. **40**(1982) 393.
- 3) I. Suemune and L. A. Coldren: IEEE J. Quantum Electron. **QE-24**(1988) 1178.
- 4) P. M. Petroff, A. C. Gossard, R. A. Logan, and W. Wiegman: Appl. Phys. Lett. **41**(1982) 635.
- 5) P. M. Petroff, A. C. Gossard, and W. Wiegman: Appl. Phys. Lett. **45**(1984) 620.
- 6) J. Cibert, P. M. Petroff, G. J. Dolan, S. J. Pearton, A. C. Gossard, and J. H. English: Appl. Phys. Lett. **49**(1986) 1275.
- 7) T. Hirayama, S. Tarucha, Y. Suzuki, and H. Okamoto: Phys. Rev. **B37**(1988) 2774.
- 8) M. A. Reed, J. N. Randall, R. J. Aggarwal, R. J. Matyi, T. M. Moore, and A. E. Wetsel: Phys. Rev. Lett. **60**(1988) 535.
- 9) M. Tsuchiya, J. M. Gaines, R. H. Yan, R. J. Simes, P. O. Holtz, L. A. Coldren, and P. M. Petroff: Phys. Rev. Lett. **62**(1989) 466.
- 10) T. Fukui and S. Ando: Electron. Lett. **25**(1989) 410.
- 11) K. Ismail, D. A. Antoniadis, and H. I. Smith: 47th Annual Device Research Conference (Cambridge, Massachusetts 1989) IVB-6.
- 12) J. M. Gaines, P. M. Petroff, H. Kroemer, R. J. Simes, R. S. Geels, and J. H. English: J. Vac. Sci. Tech. **B6**(1988) 1378.
- 13) P. M. Petroff, J. M. Gaines, M. Tsuchiya, R. J. Simes, L. A. Coldren, H. Kroemer, J. H. English, and A. C. Gossard: J. Crystal Growth **95**(1989) 260.
- 14) T. Fukui and H. Saito: Appl. Phys. Lett. **50**(1987) 824.
- 15) T. Fukui and H. Saito: J. Vac. Sci. Tech. **B6**(1988) 1373.
- 16) Y. Horikoshi, M. Kawashima, and H. Yamaguchi: Jpn. J. Appl. Phys. **25**(1986) L868.
- 17) Y. Horikoshi, M. Kawashima, and H. Yamaguchi: Jpn. J. Appl. Phys. **27**(1988) 169.
- 18) M. Tsuchiya, P. M. Petroff, and L. A. Coldren: Appl. Phys. Lett. **54**(1989) 1690.
- 19) A. Zunger: Phys. Rev. **B24**(1981) 4372.
- 20) H. Sakaki, K. Wagatsuma, J. Hamasaki, and S. Saito: Thin Solid Films **36**(1976) 497.
- 21) Y. C. Chang, L. L. Chang, and L. Esaki: Appl. Phys. Lett. **47**(1985) 1324.
- 22) E. O. Kane: J. Phys. Chem. Solids **1**(1957) 249.
- 23) Y. Arakawa, K. Vahala, and A. Yariv: Surf. Sci. **174**(1986) 155.
- 24) A. Yariv: Appl. Phys. Lett. **53**(1988) 1033.
- 25) H. Zarem, K. Vahala, and A. Yariv: IEEE J. Quantum Electron. **QE-25**(1989) 705.